Macromolecules

ARTICLE

pubs.acs.org/Macromolecules

Microgel Heterogeneous Morphology Reflected in Temperature-Induced Volume Transition and ^{1}H High-Resolution Transverse Relaxation NMR. The Case of Poly(*N*-vinylcaprolactam) Microgel

Andreea Balaceanu, Dan E. Demco,* Martin Möller, and Andrij Pich*

Functional and Interactive Polymers, DWI RWTH Aachen University, Pauwelsstrasse 8, D-52074 Aachen, Germany

Supporting Information

ABSTRACT: The Flory temperature-induced volume transition theory for homopolymer microgels was generalized for the case of bimodal heterogeneous morphology. The most probable morphological parameters were selected from the microscopic and thermodynamic constraints imposed by ^{1}H transverse relaxation NMR and Flory equation of state in the approximation of a homogeneous morphology. Proton transverse magnetization relaxation NMR proved directly the existence of a bimodal heterogeneous morphology of the PVCL microgel particle. The volume polymer fractions in the deswollen state and the number of subchains for the core and corona were obtained from size−temperature data for a series of differently cross-linked microgels made of poly(*N*-vinylcaprolactam) (PVCL) in water. The cross-link density effect given by the different amounts of cross-linker used was investigated using dynamic light scattering. From the combination of Flory heterogeneous theory and NMR transverse relaxation, the number of polymer subchains in core and corona was shown to increase with the amount of cross-linker. Moreover, the ratio of the cross-link density in core and corona could be evaluated from the transverse relaxation times T_2 of each decay components. The quantitative characterization of PVCL microgels by size−temperature data and ^{1}H transverse relaxation NMR shows the consistency of the assumptions made in the generalization of Flory theory of microgels for heterogeneous morphology.

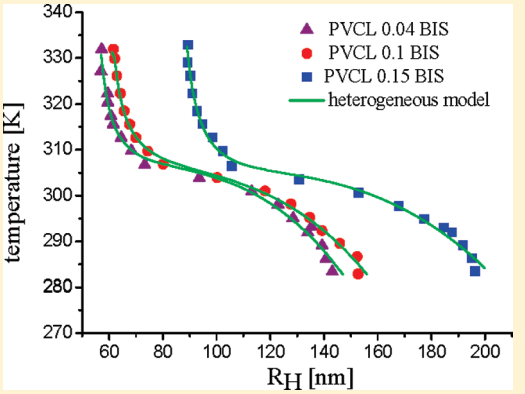

INTRODUCTION

Materials of micro/nanosize dimensions often show unique characteristics which are not expected from the bulk. For this reason, studies on such micro/nanomaterials are attracting a lot of attention and are widely extending into diverse fields of science and technology. In this way, when focusing into the polymer area, microgels are currently becoming the focus of considerable scientific studies.

Microgel particles are cross-linked polymeric particles with dimensions in the colloidal range. A promising feature deriving from their microsize is their rather fast capability to swell compared to the macroscopic gels. This is one of the reasons why these materials have generated an increasing interest in the past decades, particularly stimulus-responsive microgels. These microgels are able to alter their volume and properties in response to external stimuli, such as pH, temperature, pressure, and ionic strength. This fact proved them to be attractive candidates for many potential applications including drug delivery, biosensing, or separation techniques.[1,2]

Special interest is focused on the hydrogels based on polymers, which have a lower critical solution temperature (LCST) near the temperature of the human body. The temperature-responsive nature of these polymers leads to a variety of biological applications. Hydrogels made from these polymers have been considered as drug delivery devices, materials for tissue engineering, and materials for preventing surgical adhesion. Poly(*N*-isopropylacrilamide) (PNIPAAm) is the most widely studied hydrogel and has a LCST of 34 °C (ref 3 and references therein). Our systems are based on poly(*N*-vinylcaprolactam) (PVCL), which also has the LCST in the physiological range of around 32 °C. It is biocompatible and materials based on this polymer can be potentially used in biomedical applications.

The attempts to determine the structure of aqueous microgel particles have been reported in the literature. Wu and Pelton[4] reported that during the formation of poly(NIPAM) particles by precipitation polymerization the cross-linking agent (bis-(acrylamide)) was consumed faster compared to NIPAM and therefore preferentially incorporated into microgels. Because of the fact that poly(NIPAM) or poly(VCL) microgel particles are prepared at above the LCST of the linear polymer, it is believed that the core regions of the final particles contain a relatively higher amount of the monomers consumed in the early

Received: January 15, 2011
Revised: February 20, 2011
Published: March 10, 2011

stages of the polymerization process. Both effects contribute to the development of the heterogeneous structure within the microgel particles. The general concept for microgel structure is a core/corona model in which the core and corona, separated by diffuse boundaries, have different structures and cross-linking degree. The heterogeneous microgel structure was investigated by using static light scattering[5] and small-angle neutron scattering.[6−9]

The structural inhomogeneities inside microgel particles consisting of poly(*N*-isopropylmethacrylamide) (PNIPMAAm) were studied using ^{1}H NMR transverse relaxation measurements.[10] Different structural regions were distinguished by their different proton mobilities detected. The internal particle structure was detected to be heterogeneous. Proton transverse relaxation measurements were also used to characterize the phase transition occurring in three different types of PNIPAAm gels.[11] A short transverse relaxation value is ascribed to the restricted chain segments, and the component with a long tranverse relaxation value corresponds to the highly mobile segments. Our previous results on an amphoteric microgel, obtained by copolymerization of *N*-vinylcaprolactam (VCL), itaconic acid dimethyl ester (IADME), and vinylimidazole (VIm), using ^{1}H high-resolution site selective transverse relaxation NMR also showed a bimodal transverse relaxation behavior indicating a heterogeneous core−corona internal structure.[12]

Efforts were made in order to describe the swelling behavior of microgels using improvements on the Flory's thermodynamic theory for gel systems.[13,14] The Sanchez and Lacombe's lattice-fluid model which considers holes in the lattice as a component was used to describe the free energy of mixing, and then the model was compared with the swelling data.[15,16] A simple model in which the polymer−solvent interaction parameter depends not only on the temperature but also on the concentration of polymer was also suggested.[17] A combination of the extended Flory−Huggins model[18,19] for mixing solvent and network with a modified Flory−Rehner theory[20] for elastic contribution was used and fitted to experimental data obtained for submicrometer gel particles and bulk gels.[21] They also generalized the model for homopolymer gel particles to the copolymer gel/solvent systems by modifying the Flory interaction parameter.[22] Recently, the pressure dependence of the Flory solvency parameter was obtained by comparing the pressure- and temperature-induced deswelling.[23]

In this work we are extending the classical Flory swelling/deswelling volume transition theory applied to homopolymer microgels in order to account for the bimodal internal structural heterogeneities of the cross-linking density observed in PVCL microgels in combination with high-resolution ^{1}H transverse relaxation NMR measurements. This approach allows characterizing quantitatively the core−corona morphology of a series of PVCL microgels with different amount of cross-linker.

EXPERIMENTAL SECTION

Microgel Synthesis. *N*-Vinylcaprolactam (VCL) was purified by distillation under vacuum. Cationic surfactant *N*-cetyl-*N*,*N*,*N*-trimethylammonium bromide (CTAB), initiator 2,2′-azobis(2-methylpropionamidine) dihydrochloride (AMPA), cross-linker *N*,*N*′-methylenebis-(acrylamide) (BIS) (Aldrich), and D_2O (99.9%, KMF GmbH, Germany) were used as received.

The series of cross-linked PVCL microgels were prepared in the following way: 2.215 g of VCL; 0.022 g of CTAB; and 0.04, 0.1, and 0.15 g of BIS were dissolved in 145 g of deionized water and than placed into double-wall glass reactor equipped with mechanical stirrer. After 1 h of the incubation at 70 °C and nitrogen purging, 0.05 g of AMPA dissolved in 5 g of water was added under continuous stirring for initiation of the reaction. The reactions were carried out for 8 h. Stable microgel dispersions were obtained and were purified by dialysis (Millipore Labscale TFF System). The PVCL microgels with three different amounts of cross-linker will be referred to in the text as PVCL 0.04 BIS, PVCL 0.1 BIS, and PVCL 0.15 BIS.

Dynamic Light Scattering. The volume phase transition of the particles was monitored as particles size changes using dynamic light scattering (DLS). A Malvern Zetasizer Nano system equipped with a 4 mW helium−neon laser (λ = 633 nm) was employed, with the backscattering angle set at 173°. The temperature was controlled to a precision of ±0.1 °C. The dispersions were diluted sufficiently to diminish any colloidal interaction, as well any multiple scattering.

The time autocorrelation function, related to the normalized first-order electric field time correlation function, provides a direct means to determine the diffusion coefficient D in dilute monodisperse solutions[14]

$$\langle I(q,0)I(q,t)\rangle = \langle I(q,0)\rangle^2 + [\langle [I(q,0)]^2\rangle - \langle I(q,0)\rangle^2] \exp(-2q^2Dt) \quad (1)$$

where $I(q,t)$ is the instantaneous scattering intensity, q is the magnitude of the wavevector, and D is the translational diffusion coefficient.

In practice, the autocorrelation function is fit to a simple expression with three fitting parameters—the amplitude A, the baseline B, and the diffusion coefficient D

$$\langle I(q,0)I(q,t)\rangle = [A \exp(-q^2Dt)]^2 + B \quad (2)$$

It is crucial to realize that the baseline at long times has to equal the square of the mean static intensity, i.e., $B = \langle I(q,0)\rangle^2$. If this criterion is not realized, then artifacts such as dust are influencing the data.

Dynamic light scattering devices derive the mean diffusion coefficient from the intensity autocorrelation function using cumulant analysis and convert it into mean particle size via the Stokes−Einstein equation for spherical particles

$$R_H = \frac{k_B T}{6\pi\eta_S D} \quad (3)$$

where R_H is the hydrodynamic radius, k_B is the Boltzmann constant, and η_S is the solvent viscosity.

NMR Experiments. Proton high-resolution NMR spectrum of VCL monomer was measured using an AV600 Bruker NMR spectrometer. The microgel ^{1}H NMR spectra under magic-angle sample spinning (MAS) conditions were measured on wide-bore AV700 Bruker NMR spectrometer operating at 700 MHz with a cross-polarization magic-angle sample spinning (MAS) probe head. The rotor frequency and the sample temperature were ν_R = 7 kHz and 22 °C, respectively. The temperature was maintained within ±0.5 K, following a standard calibration. For all measurements the recycle delay was 5 s, the radio-frequency pulse length was 3.2 μs, and the dwell time was 10 μs.

The high-resolution MAS transverse relaxation (T_2) NMR measurements[24] were made at 700.2378 MHz proton frequency of Bruker AV700 NMR spectrometer. For these measurements 2 wt % of the series of microgels dissolved in deuterated water was used. The same rotor frequency, recycle delay, dwell time, and temperature as for ^{1}H spectra were employed. The decay of transverse magnetization relaxation was measured using Hahn-echo pulse sequence: $90°_x-t-180°_x-t-$Hahn echo−(acquisition), where t is the echo time.[24] Half of the Hahn echo decay was detected and Fourier transformed. The normalized integral intensity of various resonances was fitted by two-exponential decay functions using Origin 6.0 program. The errors of the fits were smaller than 10%.

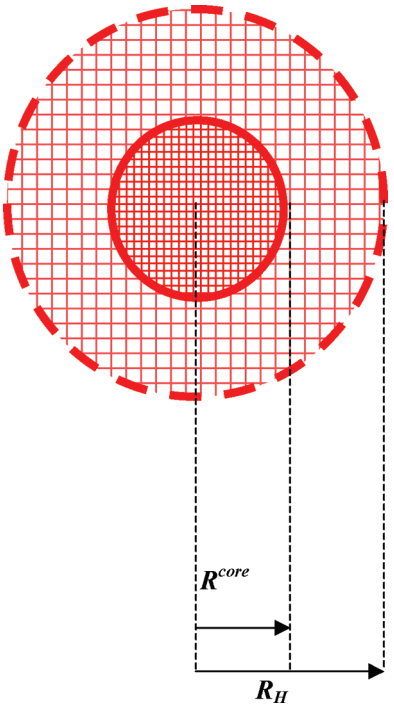

Figure 1. Bimodal morphology model for the homopolymer microgel particle.

THEORY

Flory−Rehner Theory for Homogeneous Microgel Morphology. The major hypothesis of the Flory−Rehner gel swelling theory[20] is that the free energy change on swelling consists of two contributions, which are assumed to be separable and additive. These are the energy of mixing and the free energy of elastic deformation. For a neutral microgel, the osmotic pressure arises from two major contributions: the mixing of the polymer and the solvent and the elasticity resulting from cross-linking the polymer to form the polymer network.

According to Flory's theory for the swelling of polymer gels, the equilibrium is achieved when the chemical potential of the solvent inside and outside the microgel become equal, or equivalently, when the net osmotic pressure is equal to zero, i.e.

$$\Pi = \Pi_{mix} + \Pi_{elastic} = 0 \tag{4}$$

where

$$\Pi_{mix} = -\frac{N_A k_B T}{\nu_S}[\phi + \ln(1-\phi) + \chi\phi^2] \tag{5}$$

and

$$\Pi_{elastic} = \frac{N k_B T}{V_0}\left[\left(\frac{\phi}{2\phi_0}\right) - \left(\frac{\phi}{\phi_0}\right)^{1/3}\right] \tag{6}$$

In the above equations, N_A is the Avogadro number, k_B is the Boltzmann constant, $\nu_S = 1.81 \times 10^{-5}$ m^3 is the molar volume of D_2O, which is our solvent, χ is the Flory parameter that accounts for the solubility of the polymer in the solvent, ϕ is the polymer volume fraction in the particle, N is the number of subchains in a microgel particle, and $V_0 = 4\pi R_{H0}^3/3$.

For a microgel that swells isotropically, we can write

$$\frac{\phi}{\phi_0} = \left(\frac{R_H}{R_{H0}}\right)^3 \tag{7}$$

where we choose R_H (R_{H0}) and ϕ (ϕ_0) as the particle size and volume fraction in the swollen (deswollen) state.

In order to account for the steep or discrete volume transition, the polymer−solvent interaction parameter χ is assumed to be concentration dependent and has the approximate form[17]

$$\chi \approx \chi_0 + \phi\chi_1 \tag{8}$$

with

$$\chi_0 = \frac{\Delta H - T\Delta S}{k_B T} = \frac{1}{2} - A\left(1 - \frac{\Theta}{T}\right) \tag{9}$$

where ΔS and ΔH are the corresponding entropic and enthalpic changes associated with this process, $A = (2\Delta S + k_B)/2k_B$, and $\Theta = 2\Delta H/(2\Delta S + k_B)$ is the Θ-temperature of the polymer−solvent system; for $T = \Theta$, $\chi = 0.5$ and the second virial coefficient of the mixture becomes zero.

The temperature dependence of the microgel size is accounted for through the temperature dependence of χ. By introducing eqs 7 and 8 into eq 4, we obtain an explicit equation of state relating the temperature with the hydrodynamic radius R_H[23]

$$T_{\Pi=0} = A\Theta\phi_0^2\left(\frac{R_{H0}}{R_H}\right)^6 \Big/ \left\{\frac{\nu_S N}{N_A V_0}\left[\frac{1}{2}\left(\frac{R_{H0}}{R_H}\right)^3 - \left(\frac{R_{H0}}{R_H}\right) - \phi_0\left(\frac{R_{H0}}{R_H}\right)^3 - \ln\left(1 - \phi_0\left(\frac{R_{H0}}{R_H}\right)^3\right) + \left(A - \frac{1}{2}\right)\phi_0^2\left(\frac{R_{H0}}{R_H}\right)^6 - \chi_1\phi_0^3\left(\frac{R_{H0}}{R_H}\right)^9\right\}\right] \tag{10}$$

One major assumption employed in the derivation of the above equation of state is the uniform distribution of cross-link density throughout the microgel particle.

Flory Theory for Heterogeneous Microgel Systems. Previous studies[4−12] on microgel systems synthesized by precipitation polymerization processes have shown proof of heterogeneous internal structure due to the difference in cross-link density from core to shell. Our ^{1}H high-resolution NMR transverse relaxation measurements made on previous copolymer systems based on PVCL[12] and on the system under investigation (see below) reveal a heterogeneous cross-link density from core to corona that can be described in a good approximation by a bimodal model.

In order to describe the behavior of the bimodal heterogeneous microgel system in the Flory−Rehner formalism, we considered the mixing and elastic contributions for the core and the corona of the microgel as

$$\Pi_{mix} = \Pi_{mix}^{core} + \Pi_{mix}^{corona} \tag{11}$$

and

$$\Pi_{elastic} = \Pi_{elastic}^{core} + \Pi_{elastic}^{corona} \tag{12}$$

The heterogeneous morphology model discussed here is based on the following assumptions:

(i) The core radius shrinks with temperature proportionally with the measured hydrodynamic radius of the entire particle: $R^{core}(T) = \rho R_H(T)$ (see Figure 1), which means that in the

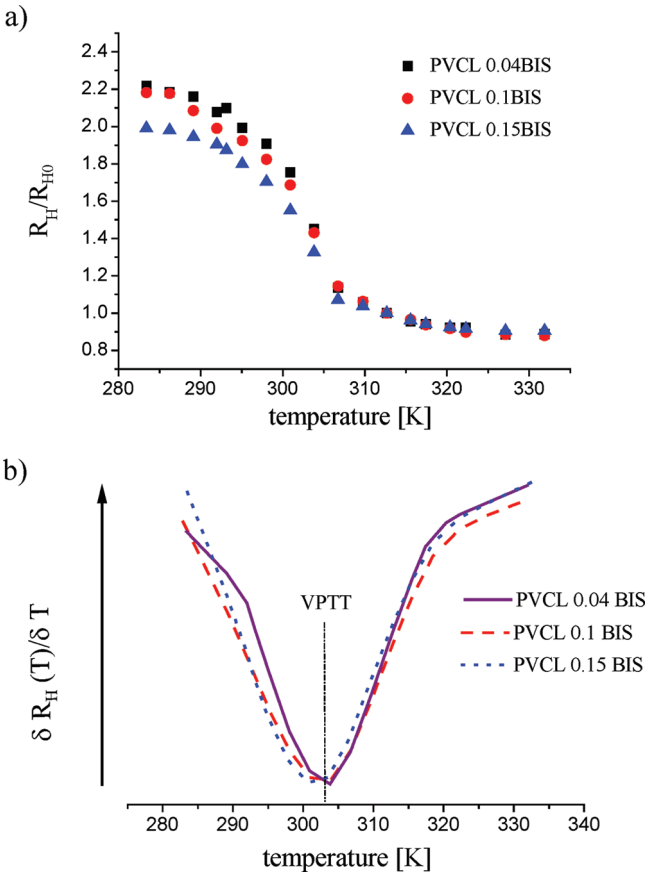

Figure 2. (a) DLS normalized hydrodynamic radius of the PVCL microgels (0.04 BIS, 0.1 BIS, and 0.15 BIS) versus temperature. (b) First-order derivatives of the volume size−temperature curves (a) showing the volume transition temperature.

deswollen state $R_0^{core} = \rho R_{H0}$. The scaling quantity ρ is assumed independent of temperature. That results in the equality of the ratios

$$\frac{\phi^{core}}{\phi_0^{core}} = \frac{\phi^{corona}}{\phi_0^{corona}} = \left(\frac{R_{H0}}{R_H}\right)^3 \quad (13)$$

The validity of this assumption will be discussed below. Nevertheless, for poly(NIPAM) microgel it was shown using SANS that the corona size evolution with temperature is different from that of the core.[6] Furthermore, this effect was not reported by the results of ref 9.

(ii) The temperature-dependent part of the Flory−Huggins interaction parameter is not influenced by the change in cross-link density from core to corona, whereas the concentration dependent part is different for the core and corona, i.e.

$$\chi^{core} = \frac{1}{2} - A\left(1 - \frac{\Theta}{T}\right) + \chi_1 \phi^{core} \quad (14)$$

and

$$\chi^{corona} = \frac{1}{2} - A\left(1 - \frac{\Theta}{T}\right) + \chi_1 \phi^{corona} \quad (15)$$

(iii) We consider that the number of subchains for the core and corona is N^{core} and N^{corona}, respectively, as a result of bimodal cross-link density model.

(iv) We neglect any elastic force of interaction between core and corona.

(v) Any defects of the polymer network such as the dangling chain and loops are not taken into account.

Considering the above assumptions, the mixing and the elastic osmotic pressures can be written as

$$\Pi_{mix} = -\frac{N_A k_B T}{\nu_S}\left\{X + \ln\left(\left[1 - \phi_0^{core}\left(\frac{R_{H0}}{R_H}\right)^3\right]\left[1 - \phi_0^{corona}\left(\frac{R_{H0}}{R_H}\right)^3\right]\right) + Y\left[\frac{1}{2} - A\left(1 - \frac{\Theta}{T}\right)\right] + Z\chi_1\right\} \quad (16)$$

and

$$\Pi_{elastic} = \frac{k_B T}{V_0}\left[\frac{1}{2}\left(\frac{R_{H0}}{R_H}\right)^3 - \frac{R_{H0}}{R_H}\right]\left[\frac{N^{core}}{\rho^3} + \frac{N^{corona}}{1-\rho^3}\right] \quad (17)$$

where X, Y, and Z are defined as

$$X = \left(\frac{R_{H0}}{R_H}\right)^3 (\phi_0^{core} + \phi_0^{corona})$$

$$Y = \left(\frac{R_{H0}}{R_H}\right)^6 [(\phi_0^{core})^2 + (\phi_0^{corona})^2] \quad (18)$$

and

$$Z = \left(\frac{R_{H0}}{R_H}\right)^9 [(\phi_0^{core})^3 + (\phi_0^{corona})^3]$$

By matching these two terms in the equation of state, we get the hydrodynamic radius−temperature dependence ($R_H(T)$), i.e.

$$T_{\Pi=0} = YA\Theta / \left\{\frac{\nu_S}{V_0 N_A}\left[\frac{1}{2}\left(\frac{R_{H0}}{R_H}\right)^3 - \left(\frac{R_{H0}}{R_H}\right)\right]\left[\frac{N^{core}}{\rho^3} + \frac{N^{corona}}{1-\rho^3}\right] - X - \ln\left(\left[1 - \phi_0^{core}\left(\frac{R_{H0}}{R_H}\right)^3\right]\left[1 - \phi_0^{corona}\left(\frac{R_{H0}}{R_H}\right)^3\right]\right) + Y\left(A - \frac{1}{2}\right) - Z\chi_1\right\} \quad (19)$$

Finally, we can note that the equation of state for a homopolymer microgel with bimodal heterogeneity given by eq 19 in the limit of $N^{corona} \to 0$, $\phi_0^{corona} \to 0$, and $\rho \to 1$ agrees with the equation of state derived for the homogeneous morphology (eq 10).

RESULTS

Dynamic Light Scattering Study on the Effect of Cross-Linker Amount. Figure 2a shows the temperature-dependent swelling of the PVCL microgels prepared with different amount of cross-linker. In order to compare the swelling behavior of the three samples, the measured hydrodynamic radius (R_H) is normalized by the value in the deswollen state (R_{H0} at 40 °C). The cross-link density has an effect on the swelling behavior of the particles—the relative swelling of the microgel particles decreases with the increase of cross-linker amount used in synthesis, which means that the microgel particles become more compact and the network loses elasticity and permits less uptake

dx.doi.org/10.1021/ma200103y |*Macromolecules* 2011, 44, 2161–2169

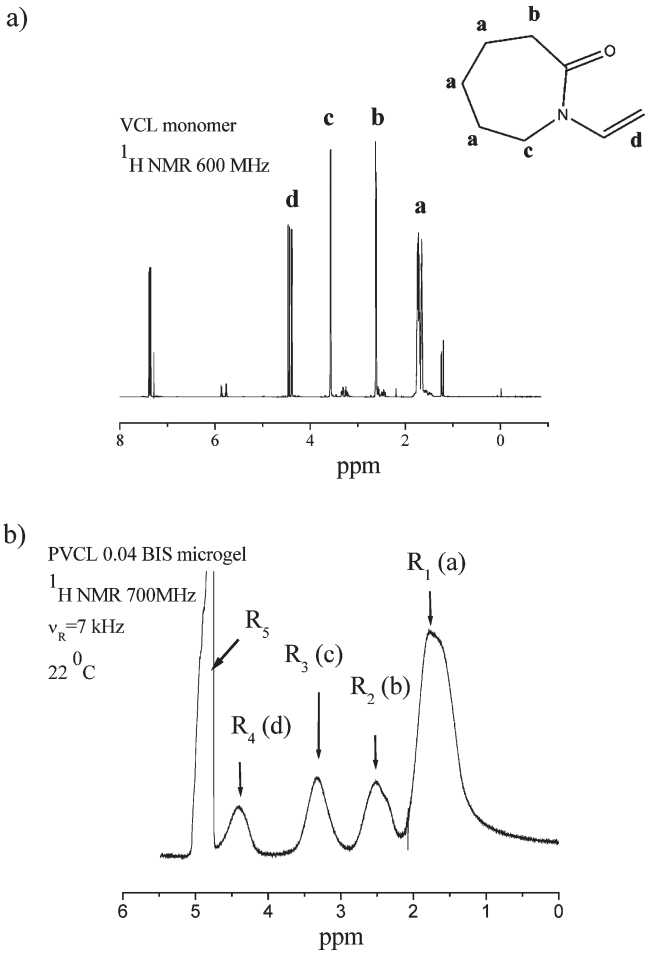

Figure 3. (a) Proton high-resolution of VCL monomer in D_2O measured at 600 MHz. The resonance's assignments are shown in the scheme using NMR spectrum simulations. (b) Proton high-resolution spectrum of PVCL microgel (2 wt % in D_2O) at 22 °C. The spectrum was measured at 700 MHz with a NMR spectrometer under MAS conditions (ν_R = 7 kHz).

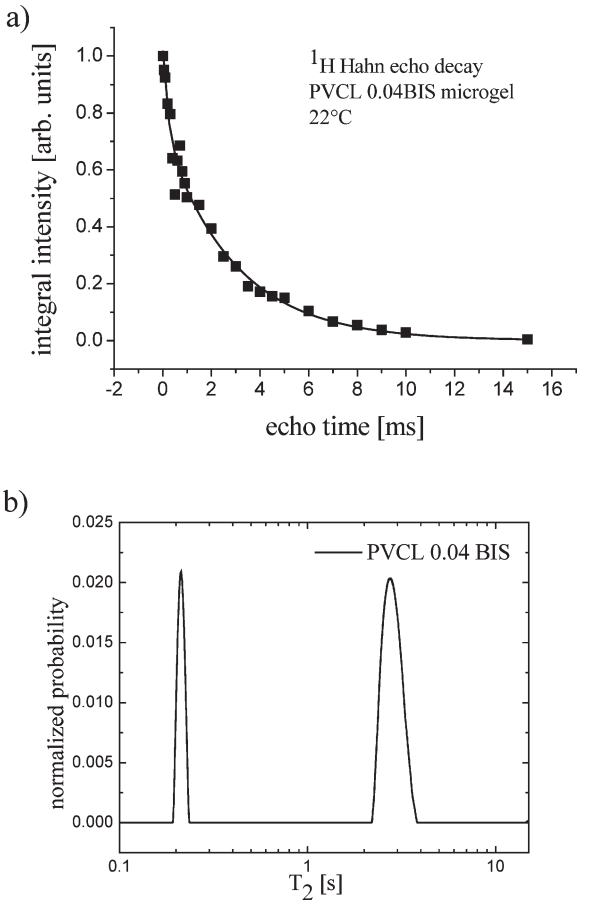

Figure 4. (a) Proton NMR transverse relaxation decay by Hahn echo for 0.04 BIS PVCL microgel at 22 °C with concentration of 2% in D_2O fitted with biexponential decay function (solid line). (b) Inverse Laplace transformation of the NMR experimental data from (a) shows the existence of two decay components.

of water. Nevertheless, this decrease of the swelling of the microgel particles is not drastic, and for the first two microgel systems (PVCL 0.04 BIS and 0.1 BIS), although the cross-linker amount is double, the swelling remains almost constant. Figure 2b shows the first-order derivative of the temperature transition curves measured by DLS. As it can be seen, the volume phase transition temperature shows only a slight dependence on the amount of cross-linker of the PVCL microgels. These findings are in agreement with other investigations on PNIPAM microgels.[5,25] We also mention that the size of the microgel particles increases with the increase of the cross-linker amount, a phenomenon not observed for PNIPAM microgels.

Structure and Dynamic Heterogeneity of Microgels by ^{1}H Transverse Magnetization Relaxation. To confirm the bimodal heterogeneous structure of the homopolymer microgels of PVCL, we performed an NMR study using ^{1}H high-resolution spectroscopy and relaxometry. Proton high-resolution NMR spectrum of VCL monomer measured at 600 MHz is shown in Figure 3a. The assignment of these peaks (see scheme in Figure 3a) was made by comparison with simulated NMR spectra obtained using the ChemDraw and Gaussian03 programs. The proton high-resolution spectrum of PVCL 0.04 BIS microgel measured in D_2O at 22 °C with an AV700 Bruker NMR spectrometer under MAS condition (rotor frequency of 7 kHz) is shown in Figure 3b. The deformation effect by centrifugal forces on microgels should broaden the resonances and was not detected at this rotor frequency. In the resulting NMR spectrum we have identified resonances with the following chemical shifts: R_1 = 1.8 ppm, R_2 = 2.5 ppm, R_3 = 3.3 ppm, R_4 = 4.4 ppm, and R_5 = 4.8 ppm. The R_5 resonance corresponds to HDO, while the others were assigned to different proton groups in the microgel (Figure 3a). In the limit of experimental errors the amount of cross-linking will not modify the resonances assignment. Resonance R_1 of methylene protons was used in the following measurements to investigate the heterogeneity of the PVCL microgels (see below).

The heterogeneity in the microgel particle morphology would be reflected in the ^{1}H transverse magnetization relaxation due to different degree of local molecular motions correlated to the distribution in cross-link density inside the particle.[12] From transverse magnetization (T_2) decay we can show that a bimodal distribution of molecular dynamics is present inside the microgel particle from which the morphological model of core−corona could be derived. We calculated the proton Hahn-echo decays for the individual resonances assigned in the NMR spectrum and for the ensemble of microgel resonances (Figure 3b). Because the

dx.doi.org/10.1021/ma200103y |*Macromolecules* 2011, 44, 2161–2169

Table 1. Proton Transverse Relaxation Rates Measured Using the NMR Resonance R_1 (Figure 2b) and Relative Weights Coefficients (C_S and C_L) for the Series of PVCL Microgels with Different Cross-Linker Amounts

	0.04 BIS	0.1 BIS	0.15 BIS	average
T_{2S} [ms]	0.21	0.24	0.24	0.23
C_S	0.28	0.28	0.25	0.27
T_{2L} [ms]	2.9	2.84	2.86	2.87
C_L	0.74	0.75	0.77	0.75

results are identical in the limit of experimental errors (see Table S1 in the Supporting Information), we chose to use in subsequent calculations the transverse relaxation decays of the R_1 resonance of VCL microgels because its high intensity makes it less sensitive to noise interference. The decay of PVCL 0.04 BIS microgel is shown in Figure 4a. We assume a biexponential decay for the integral intensity of R_1 resonance (Figure 4a), i.e.

$$\frac{S(t)}{S(0)} = C_S \exp\left\{-\frac{t}{T_{2S}}\right\} + C_L \exp\left\{-\frac{t}{T_{2L}}\right\} \qquad (20)$$

where $S(t)/S(0)$ is the normalized NMR signal integral as a function of spin-echo time t and C_i (i = S and L) are the relative contribution of the decays characterized by short (T_{2S}) and long (T_{2L}) transverse relaxation times. The coefficients C_S and C_L are related to the number of protons in the methylene fragments of PVCL describing quantitatively the bimodal heterogeneity of the polymer network in microgel.

The fit with two exponentials (eq 20) has $Chi^2 = 0.001\,12$ and a coefficient of correlation of $R^2 = 0.991\,12$. Moreover, to prove the existence of two decay components, we performed an inverse Laplace transform on the NMR decay curves (Figure 4b) that reveals a bimodal T_2 distribution.

The values of the ^{1}H transverse relaxation times and the relative concentration of methylene protons given by $C_{S,L}$ coefficients for the three microgel systems are shown in Table 1. The values are similar for the PVCL microgel systems with different cross-linker amounts, which means that the ratio between core and corona in terms of mobility does not change substantially with the increase of cross-linker amount in the investigated range. Therefore, we will use the average values of these parameters (Table 1) in the subsequent calculations.

It is known from the NMR relaxometry of polymer networks[26−28] that the transverse relaxation is strongly affected by the degree of the cross-link density via residual dipolar couplings and their fluctuations. Therefore, the value of $T_{2S} \approx 0.23$ ms corresponds to a network with a larger value of the cross-link density as compared to $T_{2L} \approx 2.87$ ms.

Scale invariant theory of polymer networks shows that ^{1}H transverse relaxation rate ($1/T_2$) is proportional to the averaged square of the residual dipolar Hamiltonian $\langle(\bar{H}_d)^2\rangle$, i.e.

$$\frac{1}{T_2} \propto \langle(\bar{H}_d)^2\rangle \qquad (21)$$

where the average is taken over the orientation and size of the end-to-end vector.[28,29] In the approximation of Gaussian distribution of the end-to-end vectors we can write[29]

$$\frac{1}{T_2} \propto \frac{1}{(N_{stat})^2} \qquad (22)$$

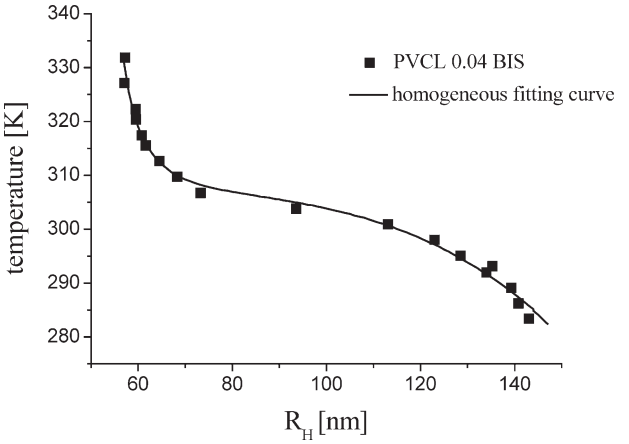

Figure 5. Size−temperature data from DLS for 0.04 BIS PVCL microgel fitted with equation of state (10) in the homogeneous morphology approximation (solid line).

Table 2. Results from the Size−Temperature Fit with Different ϕ_0 by the Homogeneous Flory Theory Morphology Approximation for PVCL 0.04 BIS Microgel (Bold Entries Correspond to the Best Fit)

ϕ_0	0.7	0.75	**0.8**	**0.85**	0.9
N	3.5×10^4	5.6×10^4	$\mathbf{8.8 \times 10^4}$	$\mathbf{1.44 \times 10^5}$	2.48×10^5
Θ	308.6	308.1	**307.41**	**306.7**	305.7
A	−3.22	−4.5	**−6.44**	**−9.59**	−15.38
χ_1	0.45	0.43	**0.39**	**0.3**	0.07

where the number of statistical segments of a subchain (strand) is denoted by N_{stat}. We can define the cross-link density as CLD $\equiv 1/N_{stat}$ (see ref 29), and finally we yield $1/T_2 \propto (\mathrm{CLD})^2$. Hence, the ratio of the cross-link density of the microgel in core and corona can be obtained from the relationship

$$\frac{\mathrm{CLD}^{core}}{\mathrm{CLD}^{corona}} = \left(\frac{T_2^{corona}}{T_2^{core}}\right)^{1/2} \qquad (23)$$

Therefore, the bimodal morphology of PVCL microgel particle is characterized from eq 23, and the data shown in Table 1 by the ratio of the averaged cross-link density of $\mathrm{CLD}^{core}/\mathrm{CLD}^{corona} \approx 3.5$.

In conclusion, the biexponential decay of the R_1 resonance of PVCL microgels can be interpreted as probing the heterogeneity of the PVCL distribution and allows the evaluation of cross-link density distribution in the microgel particle. We shall mention that for nondeformed macroscopic networks at low values of cross-link density the transverse relaxation rate is reported to be proportional with the cross-link density.[30] This is not the case of the deformed swollen microgel at equilibrium. Therefore, we shall use eq 22 as a heuristic approximation based on the general argument of $1/T_2$ proportionality to the residual second moment.[26,29]

Microgel Structural Parameters for PVCL Microgels Using the Homogeneous Flory Model. In order to estimate the temperature transition parameters for the PVCL microgels with different cross-link density, we have used experimental data measured with DLS and fitted them with the equation of state (10). Since the volume fraction in the deswollen state for this polymeric microgels is unknown, we performed different fits for

Table 3. Results for the Size−Temperature Fit by the Homogeneous Flory Theory Morphology Approximation for the Series of PVCL Microgels with Different Cross-Linker Amounts (Entries Correspond to the Best Fit)

	0.04 BIS	0.1 BIS	0.15 BIS	average
ϕ_0	0.8	0.85	0.85	0.83
N	8.8×10^4	1.85×10^5	8.2×10^5	
Θ	307.41	305.6	308.3	307.1
A	−6.44	−9.3	−7.05	−7.6
χ_1	0.39	0.23	0.49	0.37

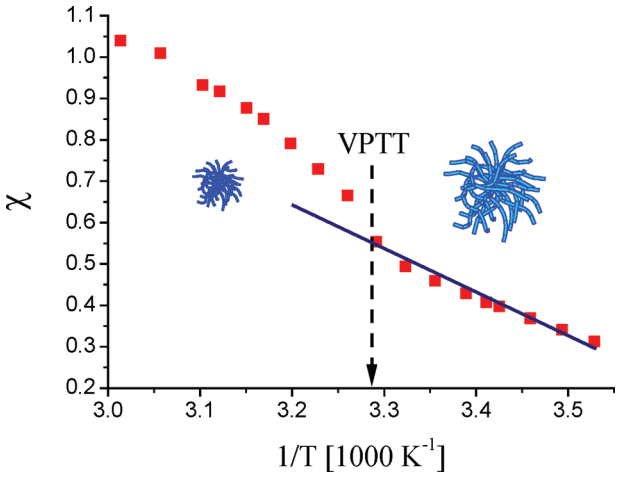

Figure 6. Temperature dependence of the Flory interaction parameter χ for the 0.04 BIS PVCL/water system using A, Θ, and χ_1 parameters from Table 2. The behavior of the interaction parameter is no longer linear above the volume phase transition temperature (VPTT).

different values of ϕ_0, leaving N, A, Θ, and χ_1 as free parameters as previously discussed in ref 23. Figure 5 shows the homogeneous model fit of the DLS data for PVCL 0.04 BIS, using the equation of state (10). The quality of different fits is comparable, the chi-square values we obtain are similar, but the resultant values for the free parameters vary considerably, as shown in Table 2 for PVCL 0.04 BIS microgel.

In order to choose the best set of values, we can compare these results with known values of the microgel parameters. We can estimate the number of subchains in the microgel particle by considering that each cross-link molecule connects two subchains. As a result $N = 2N_A V_0 c$, with c the molar concentration of the cross-linker used in the synthesis process, resulting in $N = 1.12 \times 10^5$ for PVCL 0.04 BIS. The parameters set that agrees best with this assumption are the ones for $\phi_0 = 0.8$ and $\phi_0 = 0.85$.

The best fit parameters obtained for the series of cross-linked microgels are shown in Table 3. The polymer volume fraction in deswollen state (ϕ_0), A, Θ, and χ_1 should not change with the increase of cross-linker amount, being related to the PVCL homopolymer used for the synthesis of microgels. Therefore, an average value of these parameters should be considered as standard for this type of microgels. On the other hand, the number of subchains increases with the increase of cross-linker amount.

Figure 6 shows the temperature dependence of the Flory parameter χ for the PVCL 0.04 BIS microgel, using the

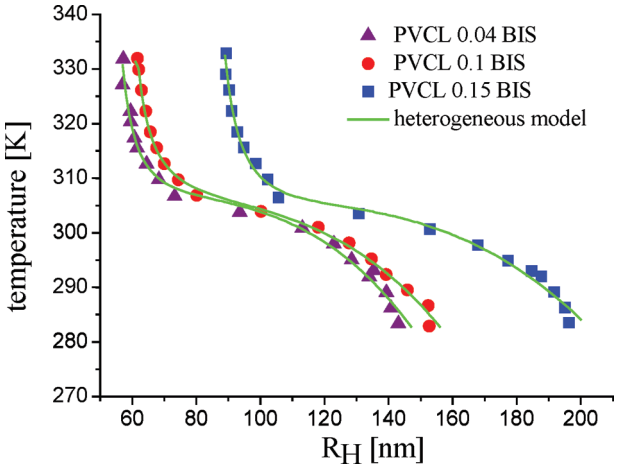

Figure 7. Size−temperature data from DLS for the series of PVCL microgels with different cross-linker amounts fitted with equation of state (eq 19) in the bimodal heterogeneous morphology approximation (solid lines).

experimental DLS measurements, eqs 8 and 9, together with the values of the best-fit parameters that we considered most accurate for $\phi_0 = 0.8$ (Table 3). Below the LCST the Flory interaction parameter scales linearly with $1/T$, but above this temperature the microgel particle deswells, and the polymer concentration dependence of the Flory interaction parameters becomes relevant, influencing the temperature dependence. As expected for a system with LCST, χ increases with temperature. Moreover, this result is in good accordance with previous literature,[31] where the value for the Flory interaction parameter for PVCL networks considering only the temperature dependence was calculated at the transition temperature of 32 °C as $\chi = 0.522$.

Considering the averaged best-fit parameters shown in Table 3, we could calculate using eq 9 parameters of interest for the PVCL polymeric microgel temperature transition. The entropic and enthalpic energies are $\Delta S = -11.18 \times 10^{-23}$ J/K and $\Delta H = -3.22 \times 10^{-20}$ J, respectively.

PVCL Microgel Structural Parameters Using the Heterogeneous Model. In order to describe the heterogeneous morphology of a microgel system, we have modified the Flory−Rehner state equation for the swelling/deswelling of microgels resulting in temperature dependence of the hydrodynamic radius given by eq 19. This equation was used to fit the data obtained by dynamic light scattering with the purpose of finding relevant microgel structural parameters (Figure 7). NMR transverse relaxation results (Table 1) were used to select the most physically correct set of fitting paramaters. Moreover, some of the microgel parameters obtained above for the homogeneous model were useful for calculating the structural parameters for the heterogeneous morphology. For instance, we can use in a good approximation the quantities A, Θ, and χ_1 determined before because the system is a homopolymer microgel. Hence, the free parameters of the fit are ϕ_0^{core}, ϕ_0^{corona}, N^{core}, N^{corona}, and ρ (see eq 19).

The best-fit set of parameters was obtained by comparing the fit quality and by comparison with the best result obtained for the homogeneous morphology model (Table 3). The best fit parameters satisfy the following conditions that relates them to the homogeneous model, i.e.

Table 4. Results for the Size−Temperature Fit for the Heterogeneous Morphology of the Series of PVCL Microgels with Different Cross-Linker Amounts, Considering the Best-Fit Results of the Homogeneous Model for the Flory Interaction Parameters[a]

	0.04 BIS	0.1 BIS	0.15 BIS	average
ϕ_0^{core}	0.8	0.85	0.85	0.83
ϕ_0^{corona}	0.8	0.85	0.85	0.83
N^{core}	2.19×10^4	3.9×10^4	1.75×10^5	
N^{corona}	1.69×10^4	3.2×10^4	1.28×10^5	
ρ	0.51	0.49	0.49	0.5

[a] These results were selected to be in quantitative agreement with the parameters of the homogenous morphology model (Table 3) and the heterogeneity showed by ^{1}H NMR transverse relaxation (Table 1 and eq 23).

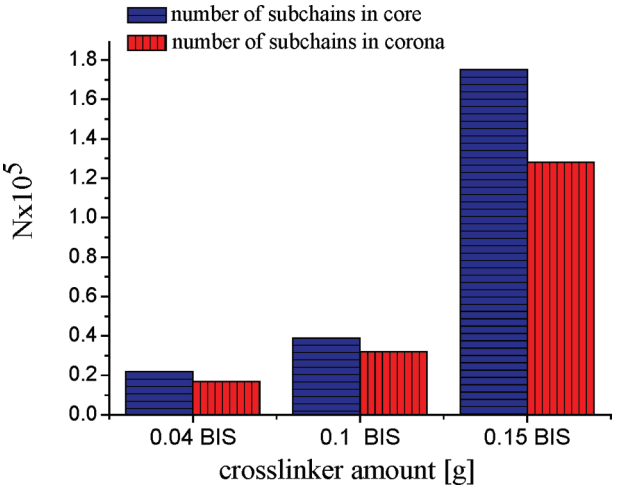

Figure 8. Dependence of the number of subchains to the cross-linker amount for the series of PVCL microgels, results obtained in the heterogeneous morphology model.

$$\frac{1}{2}\left(\frac{N^{core}}{\rho^3} + \frac{N^{corona}}{1-\rho^3}\right) = N \tag{24}$$

$$\rho^3\phi_0^{core} + (1-\rho^3)\phi_0^{corona} = \phi_0 \tag{25}$$

where N and ϕ_0 are the number of subchaines and volume fraction of gel in the deswollen state, respectively, in the homogeneous approximation.

Furthermore, we can use NMR relaxation results in order to impose additional constraints and to obtain the best-fit parameter set for the heterogeneous model. The total number of monomers (N_{mono}) in the microgel particles can be evaluated by

$$N_{mono} = mN_{stat}N \tag{26}$$

where m is the number of monomers in a statistical segment. If we assume that the number of monomers in a statistical segment will not differ in core and corona, we can write

$$\frac{N_{mono}^{corona}}{N_{mono}^{core}} = \frac{N_{stat}^{corona}}{N_{stat}^{core}}\frac{N^{corona}}{N^{core}} \tag{27}$$

The ratio of the number of monomers is proportional to the concentration of protons measured by the quantities C_i in the T_2 NMR experiment. Furthermore, from eq 22 we yield

$$\frac{C_L}{C_S}\left(\frac{T_{2S}}{T_{2L}}\right)^{1/2} = \frac{N^{corona}}{N^{core}} \tag{28}$$

The left-hand side term of the above equation can be calculated from averaged results (Table 1) of the T_2 NMR experiment (section 4.1) and has the value of ~0.8.

By taking into account all these macroscopic and microscopic constraints, we have obtained the best-fit parameters for the heterogeneous model that describes the structural heterogeneity inside the microgel particles. The results are shown in Table 4 for the series of PVCL microgels with different amount of cross-linker.

Figure 7 shows the fits of the DLS data for the series of microgels systems with different amount of cross-linker using the modified Flory temperature-induced volume transition theory (eq 19). The final results (Table 4) show the degree of structural heterogeneity inside the microgel particles. The parameter that reflects the change between the different samples investigated and inside the microgel particle is the number of subchains of core and corona for each microgel system (Figure 8). As expected, the number of subchains in both core and corona increase with the cross-linker amount. The heterogeneity inside the microgels particles is also reflected in the parameter ρ, which describes the ratio between the radius of the core and the hydrodynamic radius. The average value of $\rho \approx 0.5$ means that the volume of the core is only 12% of the total volume of the particle, while the number of subchains in the core and shell are almost equal, which reveals that the subchains density in the core and shell has a bimodal distribution.

We could mention some limitations of the NMR relaxation approach and Flory theory that *inter alia* are (i) the coefficients C_i are underestimated because of the NMR spectrometer dead time, (ii) eq 22 is valid in the approximation of Gauss distribution of the end-to-end vectors that is valid at low cross-link densities,[29] (iii) the contribution of the dipolar interaction modulation by microgel tumbling in the solvent to the transverse relaxation rate is neglected in eq 22, (iv) the dependence of χ interaction parameter on cross-link density was neglected,[32] (v) the elastic energy is overestimated in the Flory theory because the ideal chain conformation entropy is assumed, and (vi) the correlations between monomers along the polymer chain are omitted.[14]

CONCLUSIONS

The cross-linking density distribution of microgels prepared by precipitation polymerization is expected to be heterogeneous due to the specificity of the polymerization/cross-linking processes involved. This results in microgels having as a simplified model case more cross-linked core and a less cross-linked corona morphology. The discussed results show that the quantitative characterization of microgel heterogeneity is possible by size−temperature data and transverse magnetization relaxation NMR via a generalized Flory theory.

The Flory thermodynamic theory for temperature-induced volume transition of microgels was applied in the approximation of a homogeneous morphology for the series of homopolymer PVCL microgels with different amounts of cross-linker in water. The number of subchains in a microgel particle (N), polymer volume fraction in the deswolled state (ϕ_0), and the parameters

A, Θ, and χ_1 of the Flory polymer−water interaction were determined from microgel size−temperature fits measured by DLS. Therefore, the temperature dependence of the Flory interaction parameter χ for PVCL/water system was determined. Moreover, we have calculated parameters of interest for the temperature phase transition of PVCL microgels—the entropic and enthalpic energies. The effect of cross-linker amount was investigated using DLS for a series of PVCL microgel systems. The decrease of the swelling degree with cross-linker amount shows that the particles become more compact.

Proton transverse relaxation NMR experiments showed model free the existence of morphology heterogeneity in PVCL homopolymer microgels. A bimodal dynamic structure was detected with a core and corona components for the cross-linked microgel systems under investigation. Therefore, a generalization of swollen/deswollen Flory theory was proposed based on the two morphology components described by different degree of cross-linking and the assumption of temperature-independent proportionality of the core radius to the hydrodynamic microgel radius. Using this new equation of state, we have calculated heterogeneity parameters of interest for the PVCL microgel systems: ϕ_0^{core}, ϕ_0^{corona}, N^{core}, N^{corona}, and the ratio (ρ) between the measured microgel radius (R_H) and the radius of the core (R_H^{core}) (Table 4). The most probable heterogeneity parameters derived from generalized Flory theory were selected by microscopic constraints imposed by ^{1}H transverse relaxation and thermodynamic constraints derived from the homogeneous equation of state. The number of subchains for core and corona and the ratio between the radius of the core and the hydrodynamic radius reflect the degree of heterogeneity inside the particle.

The proof of validity for the equation of state (19) derived for a heterogeneous morphology stands on several arguments. In the limit when number of corona subchains goes to zero the generalized equation of state agrees with the classical Flory−Rehner relationship (eq 10). Moreover, the hydrodynamic radius−temperature data were fitted well with this new equation of state assuming Flory interaction parameters obtained by the homogeneous morphology approach. The weighted average number of subchains and polymer volume fractions obtained from the heterogeneous Flory−Rehner theory are in quantitative agreement with the values obtained based on the classical homogeneous approach. That proved *a posteriori* the validity of the assumptions made for the derivation of equation of state for a homopolymer microgel showing a heterogeneous morphology.

We can also mention that both equations of state describing homogeneous and heterogeneous structure fit in a good approximation the experimental data but with different sets of morphological parameters. The characterization of the microgel with multiple temperature-induced volume transitions based on the developed formalism will be published elsewhere.

■ ASSOCIATED CONTENT

Supporting Information. Table S1. This material is available free of charge via the Internet at http://pubs.acs.org.

■ AUTHOR INFORMATION

Corresponding Author

*E-mail: pich@dwi.rwth-aachen.de (A.P.); demco@mc.rwth-aachen.de (D.E.D.).

■ ACKNOWLEDGMENT

A.B. and A.P. acknowledge the financial support of this research by VolkswagenStiftung. We also acknowledge useful discussions with Prof. Victor Litvinov, Prof. Crisan Popescu, and Dr. Radu Fechete.

■ REFERENCES

(1) Pich, A. Z.; Adler, H. J. P. *Polym. Int.* **2006**, *56*, 291.
(2) Saunders, B. R.; Laajam, N.; Daly, E.; Teow, S.; Hu, X.; Stepto, R. *Adv. Colloid Interface Sci.* **2009**, *147−148*, 251.
(3) Karg, M.; Hellweg, T. *Curr. Opin. Colloid Interface Sci.* **2009**, *14*, 438.
(4) Wu, X.; Pelton, R. H.; Hamielec, A. E.; Woods, D. R.; McPhee, W. *Colloid Polym. Sci.* **1994**, *272*, 467.
(5) Varga, I.; Gilanyi, T.; Meszaros, R.; Filipcsei, G.; Zrinyi, M. *J. Phys. Chem. B* **2001**, *105*, 9071.
(6) Fernández-Barbero, A.; Fernández-Nieves, A.; Grillo, I.; López-Cabarcos, E. *Phys. Rev. E* **2002**, *66*, 051803.
(7) Saunders, B. R. *Langmuir* **2004**, *20*, 3925.
(8) Mason, T. G.; Lin, M. Y. *Phys. Rev. E* **2005**, *71*, 040801 (R).
(9) Stieger, M.; Richtering, W.; Pedersen, J. S.; Linder, P. *J. Chem. Phys.* **2004**, *120*, 6197.
(10) Guillermo, A.; Cohen Addad, P. J.; Bazile, J. P.; Duracher, D.; Elaissari, A.; Pichot, C. *J. Polym. Sci., Part B: Polym. Phys.* **1999**, *38*, 889.
(11) Ru, G.; Wang, N.; Huang, S.; Feng, J. *Macromolecules* **2009**, *42*, 2074.
(12) Schachschal, S.; Balaceanu, A.; Melian, C.; Demco, D. E.; Eckert, T.; Richtering, W.; Pich, A. *Macromolecules* **2010**, *43*, 4331.
(13) Flory, P. J. *Principles of Polymer Chemistry*; Cornell University Press: London, 1953.
(14) Rubinstein, M.; Colby, R. H. *Polymer Physics*; Oxford University Press: New York, 2003.
(15) Marchetti, M.; Prager, S.; Cussler, E. L. *Macromolecules* **1990**, *23*, 1760.
(16) Marchetti, M.; Prager, S.; Cussler, E. L. *Macromolecules* **1990**, *23*, 3445.
(17) Moerkerke, R.; Koningsveld, R.; Berghmans, H.; Dusek, K.; Solc, K. *Macromolecules* **1995**, *28*, 1103.
(18) Huggins, M. L. *J. Chem. Phys.* **1941**, *9*, 440.
(19) Flory, P. J. *J. Chem. Phys.* **1941**, *9*, 660.
(20) Flory, P. J.; Rehner, J. *J. Chem. Phys.* **1943**, *11*, 521.
(21) Oh, K. S.; Bae, Y. C. *J. Appl. Polym. Sci.* **1998**, *69*, 109.
(22) Oh, K. S.; Bae, Y. C. *Eur. Polym. J.* **1999**, *35*, 1653.
(23) Lietor-Santos, J. J.; Sierra-Martin, B.; Vavrin, R.; Hu, Z.; Gasser, U.; Fernandez-Nieves, A. *Macromolecules* **2009**, *42*, 6225.
(24) Ernst, R. R.; Bodenhausen, G.; Wokaun, A. *Principles of Nuclear Magnetic Resonance in One and Two Dimensions*; Clarendon Press: Oxford, 1987.
(25) Senf, H.; Richtering, W. *Colloid Polym. Sci.* **2000**, *278*, 830.
(26) Cohen Addad, J. P. *Prog. Nucl. Magn. Reson. Spectrosc.* **1993**, *25*, 1.
(27) Demco, D. E.; Hafner, S.; Spiess, H. W. In *Handbook of Spectroscopy of Rubbery Materials*; Litvinov, V., De, P. P., Eds.; Repra Technology Ltd.: Shawbury, UK, 2002.
(28) Sotta, P.; Fülber, C.; Demco, D. E.; Blümich, B.; Spiess, H. W. *Macromolecules* **1996**, *29*, 6222.
(29) Fechete, R.; Demco, D. E.; Blümich, B. *J. Chem. Phys.* **2003**, *118*, 2411.
(30) Litvinov, V. M.; Dias, A. A. *Macromolecules* **2001**, *34*, 4051 and references therein.
(31) Ilavsky, M.; Mamytbekov, G.; Sedalkova, Z.; Hanykova, L.; Dušek, K. *Polym. Bull.* **2001**, *46*, 99.
(32) Freed, K. F.; Pesci, A. I. *Macromolecules* **1989**, *22*, 4048 and references therein.